

# CNO Line Radiation and the X-ray Bowen Fluorescence Mechanism in Optically-Thick, Highly-Ionized Media

Masao Sako<sup>1</sup>

*Theoretical Astrophysics, California Institute of Technology, MC 130-33, Pasadena, CA 91125*

masao@tapir.caltech.edu

## ABSTRACT

Radiative transfer effects due to overlapping X-ray lines in a high-temperature, optically-thick, highly-ionized medium are investigated. One particular example, where the O VIII Ly $\alpha$  doublet ( $2\ ^2P_{1/2,3/2} - 1\ ^2S_{1/2}$ ) coincide in frequency with the N VII Ly $\zeta$  lines ( $7\ ^2P_{1/2,3/2} - 1\ ^2S_{1/2}$ ) is studied in detail to illustrate the effects on the properties of the emergent line spectrum. We solve the radiative transfer equation to study the energy transport of resonance line radiation in a static, infinite, plane-parallel geometry, which is used to compute the destruction/escape probabilities for each of the lines for various total optical thicknesses of the medium, as well as destruction probabilities by sources of underlying photoelectric opacity. It is found that a large fraction of the O VIII Ly $\alpha$  line radiation can be destroyed by N VII, which can result in an reversal of the O VIII Ly $\alpha$ /N VII Ly $\alpha$  line intensity ratio similar to what may be seen under non-solar abundances. Photoelectric absorption by ionized carbon and nitrogen can also subsequently increase the emission line intensities of these ions. We show that line ratios, which are directly proportional to the abundance ratios in optically thin plasmas, are not good indicators of the true CNO abundances. Conversely, global spectral modeling that assumes optically thin conditions may yield incorrect abundance estimates when compared to observations, especially if the optical depth is large. Other potentially important overlapping lines and continua in the X-ray band are also identified and their possible relevance to recent high resolution spectroscopic observations with *Chandra* and *XMM-Newton* are briefly discussed.

---

<sup>1</sup>*Chandra* Fellow

*Subject headings:* atomic processes — line: formation — radiative transfer —  
X-rays: general

## 1. Introduction

Radiative transfer effects are capable of producing line spectra that differ substantially from those emitted under optically thin conditions. As resonance line photons travel through a medium that is optically thick to its own radiation, multiple non-coherent scattering substantially alters the line profiles of the emergent spectrum. Line transfer also affects the emergent line intensities through line or continuum absorption, in which case the energy is either (1) re-radiated through other discrete transitions or (2) is used in heating the ambient gas. In hydrogen-like ions, for example, the upper levels of the higher-series Lyman transitions ( $\beta$ ,  $\gamma$ ,  $\delta$ , etc.) have finite probabilities of decaying to excited states. This implies that the Lyman line photons will be destroyed and re-radiated in the Balmer, Paschen, etc. series if the line optical depths are sufficiently large. Ratios of Lyman to Balmer line intensities, for example, can then be used to estimate the optical depth, as well as other local physical parameters, such as the density and temperature (see, e.g., Drake & Ulrich 1980, and references therein).

Another well-known example of such an effect is the Bowen fluorescence mechanism (Bowen 1934, 1935), where it was realized that the coincidence in the wavelengths of He II ( $\text{He}^+$ )  $\text{Ly}\alpha$  and O III ( $\text{O}^{2+}$ )  $2p - 3d$  transitions allows the conversion of He II  $\text{Ly}\alpha$  line photons into the upper levels of O III, which then decay to produce lines in the optical/UV band known as the Bowen lines at  $\lambda \approx 3000 \sim 4000 \text{ \AA}$ . These lines were commonly found to be extraordinarily strong in the optical spectra of planetary nebulae and Seyfert galaxies. Unno (1955) presented the first complete analysis of the He II  $\text{Ly}\alpha$  transfer and the conversion efficiencies of the Bowen lines, and demonstrated that the observed spectral properties can be reasonably well-described by this mechanism. Subsequently, Weymann & Williams (1969) presented a more detailed calculation using an exact form of the redistribution function and a realistic ionization balance calculation (see, also, Harrington 1972; Kallman & McCray 1980; Eastman & MacAlpine 1985; Netzer, Elitzur, & Ferland 1985).

In the simplest approximation generally adopted for spectral modeling, one assumes that line photons created in the gas escape the medium without any further interaction with the constituent atoms in the medium. This is generally referred to as the optically-thin limit or the coronal approximation in the context of collisionally ionized plasma. In this limit, the ionization balance is determined solely by the local temperature and is assumed to be entirely decoupled from the radiation field. The emission spectra computed under these

assumptions seem to apply fairly well to the observed X-ray spectra of a wide variety of sources including stellar coronae, supernova remnants, hot diffuse gas in starburst galaxies, and the intergalactic medium in clusters of galaxies.

For photoionized plasmas, on the other hand, codes such as Cloudy (Ferland et al. 1998) and XSTAR (Kallman & McCray 1982; Bautista & Kallman 2001) treat the transfer of X-ray lines using either the escape probability method or the assumption of complete redistribution. While these assumptions yield reasonable results for *isolated* lines with moderate line optical depths ( $\tau \lesssim 10$ ), it does not properly describe line scattering when absorption in the damping wings becomes important (i.e., for  $\tau \gtrsim 100 \sim 1000$  depending on the Voigt parameter; see, e.g., Shine, Milkey, & Mihalas 1975). Such conditions might be relevant for a wide variety of astrophysical environment including ionized surface layers of accretion disks, extended circumsource regions in AGN, and possibly shocked regions in the stellar wind of hot young stars.

The purpose of this paper is to demonstrate that radiative transfer effects can alter intensities of some of the brightest emission lines in the X-ray band, in particular, the hydrogen- and helium-like lines from carbon, nitrogen, and oxygen. Non-solar CNO abundance ratios have been inferred in a number of sources observed with the grating spectrometers on *Chandra* and *XMM-Newton*. The relativistic emission line interpretation of the *XMM-Newton* RGS spectra of the Seyfert 1 galaxies MCG–6-30-15 and Mrk 766 presented by Branduardi-Raymont et al. (2001), for example, requires the nitrogen emission lines, which are presumably formed in an optically thick accretion disk, to be much stronger than that of the oxygen line assuming solar abundance ratios (see also, Mason et al. 2003). Similarly, Kinkhabwala et al. (2002) conclude that nitrogen in the extended circumnuclear regions in the Seyfert 2 galaxy NGC 1068 is overabundant by a factor of  $\sim 3$  based on measurements of the hydrogen- and helium-like line intensities with the RGS (see also, Brinkman et al. 2002; Ogle et al. 2003). Jimenez-Garate et al. (2002) also report abnormally high nitrogen line intensities relative to those of oxygen in the RGS spectrum of the low-mass X-ray binary Her X-1, and interpreted as an overabundance of nitrogen due to H-burning by the CNO-cycle. All of the modeling, however, are based on rather simple models that do not include detailed line transfer. We show that the effects of line overlap alone can explain some of the observed anomalies, in particular the strength of the nitrogen lines, if the optical depth is large, and that detailed transfer models are required to infer accurate values for the CNO abundances with X-ray spectroscopic data. We note, however, that the theoretical model presented here is highly idealized in order to simply illustrate the general effects and describe the relevant spectroscopic details, and is certainly not adequate for quantitative comparisons with observations of complicated systems.

The paper is organized as follows. In §2, we describe the spectroscopic properties of the frequency range near the O VIII ( $O^{7+}$ )  $Ly\alpha$  doublet transitions, which contains a pair of overlapping N VII ( $N^{6+}$ )  $Ly\zeta$  lines and underlying sources of continuum opacity, which is usually dominated by K-shell absorption of H- and He-like carbon ( $C^{4+}$  and  $C^{5+}$ ) and He-like nitrogen ( $N^{6+}$ ). We compute the destruction probabilities of O VIII  $Ly\alpha$  due to line absorption by the N VII  $Ly\zeta$  transition and continuum absorption by carbon and nitrogen for temperatures ranging from cool photoionized media ( $kT \sim 10$  eV) to hot collisionally ionized plasmas ( $kT \sim 1$  keV), which is described in §3. We demonstrate that the wavelength coincidence allows efficient conversion of O VIII  $Ly\alpha$  line radiation into the N VII lines, and may be misidentified as a CNO abundance anomaly (§4). Finally, in §5, a few other potentially important overlaps are identified and their effects on the global X-ray spectrum under optically thick conditions are briefly discussed.

## 2. Spectroscopy

In the non-relativistic, hydrogenic approximation, the transition energy of the O VIII  $Ly\alpha$  line ( $n = 2 \rightarrow 1$ ) coincides exactly with that of the N VII  $Ly\zeta$  ( $n = 7 \rightarrow 1$ ) line; i.e.,  $Z_a^2(1 - 1/n^2) = Z_b^2(1 - 1/m^2)$  holds exactly for  $Z_a = 8$ ,  $n = 2$  and  $Z_b = 7$ ,  $m = 7$ . More precisely, the O VIII  $Ly\alpha$  transition is a doublet at wavelengths  $\lambda_{Ly\alpha_1} = 18.96711 \text{ \AA}$  (653.680 eV) and  $\lambda_{Ly\alpha_2} = 18.97251 \text{ \AA}$  (653.494 eV) that correspond to decays to the ground state from the  $^2P_{3/2}$  and  $^2P_{1/2}$  levels, respectively. The oscillator strength of the  $Ly\alpha_1$  line is twice that of the  $Ly\alpha_2$  line. The N VII  $Ly\zeta$  transition is also a doublet with  $\lambda_{Ly\zeta_1} = 18.97411 \text{ \AA}$  (653.439 eV) and  $\lambda_{Ly\zeta_2} = 18.97418 \text{ \AA}$  (653.436 eV). Since the wavelength difference of 0.07 mÅ is much too small to be resolved at any reasonable temperature where  $N^{6+}$  can exist, we simply treat them as a single line with an oscillator-strength-averaged wavelength of  $\lambda = 18.97413 \text{ \AA}$  (653.438 eV; see, Figure 1). The O VIII  $Ly\alpha$  and N VII  $Ly\zeta$  transition wavelengths are adopted from Johnson & Soff (1985) and Garcia & Mack (1965), respectively, which include reduced-mass and quantum electrodynamical corrections to the eigenvalues of the Dirac equation<sup>2</sup>. Oscillator strengths and radiative decay rates are calculated using the Flexible Atomic Code (FAC<sup>3</sup>; Gu 2003). All of the relevant atomic parameters are listed in Table 1.

The relative cross sections assuming solar abundances ( $A_N/A_O = 0.13$ ; Anders & Grevesse 1989) and a temperature of  $kT = 10$  eV, typical for a photoionization-dominated medium

---

<sup>2</sup>see, also the NIST Atomic Spectra Database – [http://physics.nist.gov/cgi-bin/AtData/main\\_asd](http://physics.nist.gov/cgi-bin/AtData/main_asd)

<sup>3</sup><ftp://space.mit.edu/pub/mfgu/>

at this level of ionization, are shown in Figures 2. At this temperature, the N VII Ly $\zeta$  lies approximately 2 Doppler widths away from the O VIII Ly $\alpha_2$  line and 10 Doppler widths from the Ly $\alpha_1$  line. The cross section is almost three orders of magnitude lower than that of the O VIII lines, which implies that significant scattering between the lines occur when the total optical depth is  $\gtrsim 10^3$ . Similarly, at a temperature of  $kT = 50$  eV, the N VII Ly $\zeta$  lies  $\sim 1$  Doppler width away from the O VIII Ly $\alpha_2$  line and 4 Doppler widths from the Ly $\alpha_1$  line, as shown in Figure 3.

The emission coefficient in this spectral range is dominated almost entirely by the O VIII Ly $\alpha$  lines. The intrinsic N VII Ly $\zeta$  emission coefficient is approximately two to three orders of magnitude lower in both collision-dominated and recombination-dominated plasmas with solar  $A_N/A_O$  abundance ratio. If the medium is photoionized by some external source of continuum radiation, photoexcitation may enhance the line emissivities of the N VII lines, but this is important only in the surface layer within  $\tau \lesssim 10$ , as external radiation will not be able to penetrate deeper into the medium. Since we are primarily interested in the properties of the Bowen mechanism at large optical depths, we ignore the N VII Ly $\zeta$  intrinsic source term entirely.

Absorption of an O VIII line photon by N VII is followed by one of the following two processes: (1) re-emission in the N VII Ly $\zeta$  line, which results in a pure scattering event or (2) destruction of the line through cascades via the upper levels ( $n = 2 - 6$ ), followed eventually by decay to the ground level. Collisional excitation and de-excitation from these levels are important at only extremely high electron densities ( $n_{e,\text{crit}} \sim 10^{21} \text{ cm}^{-3}$ ), and so we do not consider these processes here. We note, however, that thermalization of the line photons via collisions may occur at sufficiently high density and high optical depth, such that  $n_e \langle N \rangle_{\text{line}} \gtrsim n_{e,\text{crit}}$ , where  $\langle N \rangle_{\text{line}}$  is the mean number of scatterings experienced by the line photons as they propagate through the medium.

The branching ratios for the two possible processes can be determined from the radiative decay rates from the  $7p$  level to all possible levels. We use radiative rates calculated with FAC except for the two-photon decay rates, which are adopted from Drake (1986). The branching ratios for processes (1) and (2) are found to be 0.797 and 0.203, respectively. The final fate of the 20.3% of the line photons that initially decay to an upper level can be understood by computing the cascade matrices; quantities that represent the probabilities of one state decaying to another state via all possible channels (Seaton 1959). We find, for example, that 58% of them produce the Balmer, Paschen, etc. lines and eventually result in two-photon emission from the  $2^2S_{1/2}$  level, while the remaining 42% produce the Lyman lines in the soft X-ray band.

Continuum opacity from ions that coexist with O VIII is dominated primarily by C V

(ionization potential  $\chi = 31.622$  Å), C VI ( $\chi = 25.303$  Å), and N VI ( $\chi = 22.458$  Å) for both collisionally and photoionized plasmas in ionization and thermal equilibrium. The threshold wavelength of N VII ( $\chi = 18.587$  Å) lies shortward of the O VIII Ly $\alpha$  line. Lower charge states of carbon and nitrogen may contribute very small amounts of continuum opacity as well. For solar abundances, the typical value for the combined continuum opacity relative to the O VIII Ly $\alpha$  line opacity is  $\sim 10^{-4}$ , but can range anywhere from a few  $\times 10^{-6}$  to as high as  $\sim 10^{-3}$  depending on the level of ionization and the temperature. In ionization equilibrium, a carbon or nitrogen ion that absorbs the O VIII Ly $\alpha$  line will be photoionized, and will eventually recombine to form emission lines and continua. In a recombination-dominated plasma at a temperature of  $kT \sim 100$  eV, for example, calculations show that approximately 50% of the total number of recombinations produce one of the Lyman lines.

Under most circumstances, the Compton cross section is roughly two orders of magnitude below the continuum absorption cross section. This implies that line photons are preferentially absorbed before they are Compton scattered and, therefore, continuum absorption is the dominant mechanism that competes with the line processes. Compton scattering effects will, however, be important in extremely highly-ionized regions, where only trace abundances of bound ions can survive or in low-metallicity plasmas with abundances  $\lesssim 1\%$  solar. These will be ignored entirely in the present work.

### 3. Computational Method

To illustrate the importance of line overlap, we assume an infinite, symmetric slab with a pre-specified source distribution of line photons. In reality, dynamical effects, such as velocity gradients and turbulence, as well as inhomogeneities that exist, for example, in accretion disks complicate the problem, but we ignore them in the present study. Although resonance line scattering, in general, produces polarized light, we assume that the radiation field is unpolarized (cf., Lee, Blandford, & Western 1994). To simplify the computational procedure even further, the medium is assumed to be isothermal with a constant level of ionization. We solve the radiative transfer equation in the frequency range near the O VIII Ly $\alpha$  lines by properly accounting for scattering and absorption by the various overlapping lines, as well as the presence of a background continuum opacity source. Using the emergent intensity, we then compute the escape probabilities of the original O VIII Ly $\alpha$  line photons and conversion efficiencies into the N VII lines and photoelectric absorption as functions of the total optical depth of the slab.

The radiative transfer equations for rays propagating in the  $+\mu$  and  $-\mu$  directions ( $\mu \equiv \cos \theta$ , where  $\theta$  is the angle from the normal  $z$ -axis) in a plane-parallel medium can

be written as,

$$\pm\mu \frac{\partial I(z, \nu, \pm\mu)}{\partial z} = \sum_i k_i(\nu) [S_i(z, \nu) - I(z, \nu, \pm\mu)] \quad (1)$$

where  $\theta$  is the angle measured from the  $z$ -direction, which we define to be normal to the slab. The right-hand-side is summed over all possible sources of opacity and emissivity in the slab. We express the frequency in terms of the frequency shift from the reference line center at frequency  $\nu_0$  in units of the Doppler width  $\Delta\nu_D$ , i.e.,  $x = (\nu - \nu_0)/\Delta\nu_D$ , and write the line absorption coefficient ( $\text{cm}^{-1}$ ) as  $k_i(x) = k_{iL}\phi_a(x)$ .

Since most X-ray resonance lines have large radiative decay rates ( $A_r \gtrsim 10^{12} \text{ s}^{-1}$ ), the population of the upper level is usually negligible compared to that of the ground state. Denoting the transition oscillator strength as  $f_{ul}$  and the lower-level density as  $n_i$  ( $\text{cm}^{-3}$ ), we can then write,

$$k_{iL} = \frac{\pi e^2 f_{ul} n_i}{m_e c \Delta\nu_D}, \quad (2)$$

and  $\phi_a(x)$  is the normalized Voigt profile,

$$\phi_a(x) = \frac{H(a, x)}{\sqrt{\pi}} = \frac{a}{\pi^{3/2}} \int_{-\infty}^{\infty} \frac{e^{-t^2} dt}{(x - t)^2 + a^2}. \quad (3)$$

Adopting the notation of Hummer & Kunasz (1980), we define  $\tau$  to be the mean optical scale, which increases in the negative  $z$ -direction through the slab. Therefore,  $d\tau = -k_L dz$ , which is related to the line center optical depth  $\tau_0$  by,  $\tau_0 = \phi_a(0)\tau$ .

We assume that the continuum is purely absorbing with zero local emissivity. The source function then contains only the line terms, and can be written as (Hummer 1969),

$$S_{iL}(\tau, x) = \frac{1 - \epsilon_i}{\phi_{i,a}(x)} \int_{-\infty}^{+\infty} R(x, x') J(\tau, x') dx' + G_i(\tau), \quad (4)$$

where the first term represents the scattering term and  $G_i(\tau)$  is the intrinsic source term. The quantity  $\epsilon_i$  is the destruction probability of the line per scattering (i.e.,  $\epsilon = 0.203$  for the N VII Ly $\zeta$  line) and  $J(\tau, x)$  is the angle-averaged intensity,

$$J(\tau, x) = \frac{1}{2} \int_{-1}^{+1} I(\tau, x, \mu) d\mu. \quad (5)$$

The scattering term is computed assuming partial redistribution in a Voigt profile, in which photons scatter coherently in the atoms' frame. Compared to the assumption of complete redistribution, this provides a more accurate representation of line scattering in an optically

thick medium where scattering in the damping wings is important. The frequency redistribution function  $R(x, x')$  is defined as the probability that a photon of frequency  $x$  absorbed by an ion is re-emitted at frequency  $x'$ , and can be written as,

$$R(x, x') = \frac{1}{\pi^{3/2}} \int_{-\infty}^{+\infty} e^{-u^2} \left\{ \tan^{-1} \left[ \frac{\max(x, x') + x}{a} \right] - \tan^{-1} \left[ \frac{\min(x, x') - x}{a} \right] \right\} du, \quad (6)$$

which was first derived by Henyey (1941) (see, also Hummer 1962, and references therein). Accounting for the angular redistribution makes negligible difference (Milkey, Shine, & Mihalas 1975) and is, therefore, ignored. The intrinsic source term is frequency independent and can be produced, for example, through collisional excitation and or radiative cascades following recombination. The exact nature of the excitation mechanism is not important for our present purposes.

The transfer equation for multiple overlapping lines can then be written as,

$$\pm \mu \frac{dI_\nu(x, \mu, \tau)}{d\tau} = \sum_i \left[ I(x, \mu, \tau) \alpha_i(x) + (1 - \epsilon_i) \frac{\alpha_i(x)}{\phi_a(x)} \int_{-\infty}^{\infty} R_i(x', x) J(\tau, x') dx' + \alpha_i(x) G_i(\tau) \right], \quad (7)$$

where  $\alpha_i(x)$  represent the absorption coefficients normalized to that of the reference line at  $x = 0$ , and are assumed to be independent of depth. Therefore, the first, second, and third terms on the right hand side of Eq. 7 represent absorption, scattering, and intrinsic emission, respectively.

The transfer equation is solved using the Feautrier method (Feautrier 1964), which requires a discretized version of Eq. 7 in angular, frequency, and optical depth variables. Defining the total opacity  $\phi_{\text{tot}}(x) = \sum \phi_{i,a}(x) + \beta$ , where  $\beta$  is the continuum opacity relative to the reference line opacity ( $\beta = k_C/k_L$ ) assumed to be independent of frequency across the line, we define a mean-intensity-like quantity,

$$j_{\mu\nu} = \frac{1}{2} [I(x, +\mu, \nu) + I(x, -\mu, \nu)], \quad (8)$$

and rewrite Eq. 7 as a second order differential equation,

$$\mu^2 \frac{d^2 j_{\mu\nu}}{d\tau^2} = \phi_{\text{tot}}^2(x) j_{\mu\nu} + \phi_{\text{tot}}(x) \sum_{i=0} \alpha_i(x) S_i(\tau, x). \quad (9)$$

The presence of temperature and ion abundance gradients will introduce an additional term on the right hand side, which is ignored for simplicity. We assume a symmetric slab and specify boundary conditions on the surface and at the midplane of the slab. Assuming no incident radiation on either boundaries, they can be written as,

$$\mu \left. \frac{dj_{\mu\nu}}{d\tau} \right|_{\tau=0} = j_{\mu\nu} \quad (10)$$



on the surface and,

$$\mu \left. \frac{dj_{\mu\nu}}{d\tau} \right|_{\tau=\tau_{\text{tot}}/2} = 0 \quad (11)$$

at the midplane. These boundary conditions are also discretized using a second order method described by Auer (1967). The frequency integral is represented as a quadrature sum using Simpson’s formula with  $N_x = 100 - 200$  points depending on the temperature and the total optical depth of the slab. We use a 2-point Gaussian quadrature for the angular integral in the interval  $0 \leq \mu \leq 1$  ( $N_\mu = 2$ ). The optical depth is discretized into 12 points per dex. Extensive testing shows that the above discretization scheme yields reliable results. Energy conservation (see, e.g., Hummer & Kunasz 1980) is satisfied to within  $\sim 2\%$  for most cases studied in this paper, and is no larger than  $\sim 5\%$  even in the worst cases.

#### 4. Conversion Efficiencies

We solve the transfer equation for a source function distributed uniformly within a slab of ionized material for a range of total slab thicknesses. We define the O VIII Ly $\alpha_1$  line to be our reference line and measure frequency shifts in units of its Doppler width. The emissivities of the O VIII Ly $\alpha_1$  and Ly $\alpha_2$  lines are assumed to be proportional to their respective statistical weights of the upper levels, i.e.,  $G_{\text{Ly}\alpha_1}(\tau) = 2G_{\text{Ly}\alpha_2}(\tau)$ , which is approximately correct for both collision-dominated and recombination-dominated line emission. The absolute numerical values for the source functions are not important for the present purposes, and without any loss of generality, we can write,

$$\sum_i \int_0^{\tau_{\text{tot}}} d\tau_i G_i(\tau) \equiv 1. \quad (12)$$

The solution to Eq. 9 – 11 yields the frequency-dependent intensity at each optical depth and angular points, which can then be used to compute the mean number of scatterings for each of the lines, their mean optical scales, and the escape probabilities.

Given the normalization condition (Eq. 12), the fraction of the original photons that are absorbed by a transition with destruction probability  $\epsilon_i > 0$  can be expressed in terms of the mean number of scatterings (Hummer 1969; Hummer & Kunasz 1980). The fraction absorbed and destroyed by line  $i$  can be written as,

$$f_{iL} = \frac{\epsilon_i}{1 - \epsilon_i} \langle N \rangle_i = \frac{\epsilon_i}{1 - \epsilon_i} \int_0^{\tau_{\text{tot}}} d\tau_i \int_{-\infty}^{\infty} \phi_a(x) S_{iL}(\tau, x) dx, \quad (13)$$

where  $\langle N \rangle_i$  is the mean number of scatterings. Similarly, the fraction of photons absorbed

in the continuum can be expressed in terms of the mean optical scale  $\langle l \rangle$  (Ivanov 1973), i.e.,

$$f_C = \beta \langle l \rangle = \beta \int_0^{\tau_{\text{tot}}} d\tau \int_{-\infty}^{\infty} J(\tau, x) dx. \quad (14)$$

Finally, the fraction of photons that escape through both faces of the slab is simply,

$$f_{\text{esc}} = \int_{-\infty}^{\infty} dx \int_0^1 I(\tau = 0, x, \mu) \mu d\mu, \quad (15)$$

where  $I(\tau = 0, x, \mu)$  is the emergent intensity on the surface.

Fractional conversion efficiencies as a function of the total threshold optical depth at the O VIII edge ( $\tau_{\text{O VIII}}$ ) at temperatures of  $kT = 10$  eV and 50 eV are shown in Figures 4 and 5, respectively. The underlying continuum opacity is assumed to be  $0.1 \tau_{\text{O VIII}}$ . At  $kT = 10$  eV, the line-center cross section of the O VIII Ly $\alpha_1$  line is  $6.9 \times 10^{-16}$  cm<sup>2</sup> and is a factor of  $7.0 \times 10^3$  times larger than the corresponding continuum absorption cross section at threshold, which is assumed to be  $9.9 \times 10^{-20}$  cm<sup>2</sup> for O VIII (Verner et al. 1996). For  $\tau_{\text{O VIII}} = 1$  and  $kT = 10$  eV (Figure 4), only  $\sim 40\%$  of the O VIII Ly $\alpha$  photons escape the medium, while  $\sim 40\%$  are absorbed by N VII and  $\sim 20\%$  are absorbed by the background continuum. The total line-center opacity in the O VIII Ly $\alpha_1$  line is  $6.9 \times 10^3$ . We find the mean number of scatterings for the O VIII Ly $\alpha_1$  line to be  $2.3 \times 10^3$ , which implies that thermalization through particle collisions is relevant if the gas density is higher than  $\sim 10^{18}$  cm<sup>-3</sup> (see §2). At a temperature of  $kT = 50$  eV, the overlap between the O VIII and N VII lines is larger, and the conversion to N VII is enhanced relative to the amount absorbed in the continuum.

The temperature dependence of the conversion efficiencies can be understood from the curves plotted in Figure 6. At low temperatures, the N VII Ly $\zeta$  line lies in the wings of the O VIII Ly $\alpha$  lines and so the conversion process is relatively inefficient. As the temperature is increased, the amount of overlap between the lines increases rapidly up to a temperature of  $kT \sim 40$  eV, which is where the separation between the N VII Ly $\zeta$  and O VIII Ly $\alpha_1$  lines is approximately equal to one Doppler width. This temperature is representative of a photoionized plasma at this level of ionization. Above this temperature, the amount of line overlap increases more slowly than the temperature dependence of the line cross section, which decreases approximately as  $\propto T^{-1/2}$ , and so the efficiency drops again with temperature. Finally, we show in Figure 7 the effect of increasing the overlapping continuum opacity on the conversion efficiencies.

From the derived conversion efficiencies, one can estimate the emergent intensities of each of the lines for a given total optical depth. At  $kT = 10$  eV and a total optical depth of  $\tau_{\text{O VIII}} = 1$ , approximately 40% of the original O VIII Ly $\alpha$  photons escape through the

surfaces of the slab, 40% of them are absorbed by N VII, and the remaining 20% are absorbed in the continuum (see Figure 4). Assuming that the medium is very highly ionized consisting only of H-like carbon, nitrogen, and oxygen, and further assuming that the emission coefficient ratios of the Ly $\alpha$  lines are proportional to their abundance ratios, (i.e., CNO Ly $\alpha$  relative line intensities of 1.0 : 0.13 : 0.45), the emergent radiation field will have an O VIII Ly $\alpha$  line intensity of 0.40, a N VII Ly $\alpha$  intensity of 0.26, and a carbon line intensity of 0.55. Here, we have simply assumed that 33% of the photons absorbed by N VII result in the N VII Ly $\alpha$  line and 50% of the photons absorbed by C VI produce the C VI Ly $\alpha$  line (see §2). Therefore, the oxygen to nitrogen line ratio decreased from 7.7 to 1.5 (a factor of  $\sim 5$ ) and the oxygen to carbon line ratio decreased from 2.2 to 0.73 (a factor of  $\sim 3$ ) simply due to finite opacity effects.

We do not attempt to compute the global emergent spectrum, which requires a self-consistent calculation of the O VIII Ly $\alpha$  line source functions including a complete set of ions and a realistic ionization balance calculation. To accurately compute the emergent CNO line intensities, one must properly account for all of the processes that increase the oxygen line source function. The forest of iron L-shell line emission shortward of the O VIII edge at  $\lambda = 14.228 \text{ \AA}$  is particularly important and is likely to be the dominant contributor to the source function. A more detailed investigation will be presented in a future article.

## 5. Conclusions and Discussion

We have identified a pair of overlapping resonance lines, which alters the intensities of some of the most prominent lines in X-ray spectra of cosmic sources under optically thick conditions, analogous to the He II – O III Bowen fluorescence mechanism. A non-negligible fraction of the O VIII Ly $\alpha$  photons can be converted into N VII emission lines, which can be misinterpreted as an anomalous CNO abundance pattern. In general, oxygen emission lines will be suppressed, while both nitrogen and carbon lines will be enhanced compared to those emitted under optically thin conditions.

As briefly mentioned earlier, detections of non-solar CNO abundance ratios have been made in a variety of sources using soft X-ray data obtained with the Reflection Grating Spectrometer onboard *XMM-Newton* and the *Chandra* Low Energy Transmission Grating Spectrometer (see, e.g., Branduardi-Raymont et al. 2001; Kinkhabwala et al. 2002; Jimenez-Garate et al. 2002; Brinkman et al. 2002; Mason et al. 2003; Leutenegger, Kahn, & Ramsay 2003). In all cases, the nitrogen lines are observed to be stronger than expected relative to the oxygen lines. The carbon lines, on the other hand, are stronger in some sources and weaker in others. Although it is highly likely that non-solar overabundances play a major

role in producing the anomalous line fluxes, it is also possible that a substantial part of it is due to the Bowen mechanism described in this paper. Detailed modeling and careful inspections of other lines in the observed spectrum are required to break the degeneracy between overabundance and radiative transfer effects.

Dynamical effects, such as turbulent motion and velocity gradients, which are not included in the present calculations, may reduce or enhance the conversion efficiency of O VIII Ly $\alpha$  into N VII depending on the geometrical configuration of the ionized medium. Turbulence, for example, can suppress the efficiency if the turbulent length scale is much smaller than the mean free path of the O VIII line photons. In the presence of velocity gradients, the efficiency can be enhanced in the direction where the N VII Ly $\zeta$  line is shifted into the O VIII Ly $\alpha$  line core. These effects coupled with density inhomogeneities will complicate the problem further and must be studied carefully on a case-by-case basis.

There are a few other potentially important line overlaps in the X-ray band that are worth mentioning. For example, one of the three brightest Fe XVII lines at wavelengths of 17.096 Å, 17.051 Å, and 16.780 Å typically referred to as the M2, 3G, 3F lines (Brown et al. 1998), respectively, coincide in wavelength with the high- $n$  series lines of O VII at 17.10068 Å ( $n = 7$ ), 17.02584 Å ( $n = 8$ ), etc., and 16.786 Å ( $n = \infty$ ). In this case, O VII dominates the line opacity, while Fe XVII contributes most of the intrinsic source function. Another example is the overlap between the Fe XVIII lines at 16.071 and 16.004 Å (Brown et al. 2002) with the O VIII Ly $\beta$  lines at 16.00666 Å and 16.00552 Å. These examples are certainly not exhaustive and it is highly likely that they must all be accounted for collectively for accurately predicting the global X-ray spectrum of optically thick sources.

The author thanks Roger Blandford, Steven Kahn, and Duane Liedahl for valuable discussions, and Mingfeng Gu for his help with the Flexible Atomic Code. This work was supported by NASA through *Chandra* Postdoctoral Fellowship Award Number PF1-20016 issued by the *Chandra* X-ray Observatory Center, which is operated by the Smithsonian Astrophysical Observatory for and behalf of NASA under contract NAS8-39073.

## REFERENCES

- Anders, E. & Grevesse, N. 1989, *Geochim. Cosmochim. Acta*, 53, 197
- Auer, L. 1967, *ApJ*, 150, L53
- Bautista, M. A. & Kallman, T. R. 2001, *ApJS*, 134, 139
- Bowen, I. S. 1934, *PASP*, 46, 146
- Bowen, I. S. 1935, *ApJ*, 81, 1
- Branduardi-Raymont, G., Sako, M., Kahn, S. M., Brinkman, A. C., Kaastra, J. S., & Page, M. J. 2001, *A&A*, 365, L140
- Brinkman, A. C., Kaastra, J. S., van der Meer, R. L. J., Kinkhabwala, A., Behar, E., Kahn, S. M., Paerels, F. B. S., & Sako, M. 2002, *A&A*, 396, 761
- Brown, G. V., Beiersdorfer, P., Liedahl, D. A., Widmann, K., & Kahn, S. M. 1998, *ApJ*, 502, 1015
- Brown, G. V., Beiersdorfer, P., Liedahl, D. A., Widmann, K., Kahn, S. M., & Clothiaux, E. J. 2002, *ApJS*, 140, 589
- Drake, G. W. F. 1986, *Phys. Rev. A*, 34, 2871
- Drake, S. A. & Ulrich, R. K. 1980, *ApJS*, 42, 351
- Eastman, R. G. & MacAlpine, G. M. 1985, *ApJ*, 299, 785
- Feautrier, P. 1964, *C. R. Acad. Sci. Paris*, 258, 3189
- Ferland, G. J., Korista, K. T., Verner, D. A., Ferguson, J. W., Kingdon, J. B., & Verner, E. M. 1998, *PASP*, 110, 761
- Garcia, J. D. & Mack, J. E. 1965, *Journal of the Optical Society of America*, 55, 654
- Gu, M. F. 2003, *ApJ*, 582, 1241
- Harrington, J. P. 1972, *ApJ*, 176, 127
- Heney, L. G. 1941, *Proc. Nat. Acad. Sci.*, 26, 50
- Hummer, D. G. 1962, *MNRAS*, 125, 21
- Hummer, D. G. 1969, *MNRAS*, 145, 95

- Hummer, D. G. & Kunasz, P. B. 1980, *ApJ*, 236, 609
- Ivanov, V. V. 1973, Transfer of radiation in spectral lines (NBS Special Publication, Washington: US Department of Commerce, National Bureau of Standards, 1973, English language edition)
- Jimenez-Garate, M. A., Hailey, C. J., Herder, J. W. d., Zane, S., & Ramsay, G. 2002, *ApJ*, 578, 391
- Johnson, W. R. & Soff, G. 1985, *Atomic Data and Nuclear Data Tables*, Vol. 33, p.405, 33, 405
- Kallman, T. & McCray, R. 1980, *ApJ*, 242, 615
- Kallman, T. R. & McCray, R. 1982, *ApJS*, 50, 263
- Kinkhabwala, A., Sako, M., Behar, E., Kahn, S. M., Paerels, F., Brinkman, A. C., Kaastra, J. S., Gu, M. F., et al. 2002, *ApJ*, 575, 732
- Lee, H.-W., Blandford, R. D., & Western, L. 1994, *MNRAS*, 267, 303
- Leutenegger, M. A., Kahn, S. M., & Ramsay, G. 2002, *ApJ*, 585, 1015
- Mason, K. O., Branduardi-Raymont, G., Ogle, P. M., Page, M. J., Puchnarewicz, E. M., Behar, E., Córdova, F. A., Davis, S., et al. 2003, *ApJ*, 582, 95
- Milkey, R. W., Shine, R. A., & Mihalas, D. 1975, *ApJ*, 202, 250
- Netzer, H., Elitzur, M., & Ferland, G. J. 1985, *ApJ*, 299, 752
- Ogle, P. M., Brookings, T., Canizares, C. R., Lee, J. C., & Marshall, H. L. 2003, *A&A*, 2003, 402, 849
- Seaton, M. J. 1959, *MNRAS*, 119, 90
- Shine, R. A., Milkey, R. W., & Mihalas, D. 1975, *ApJ*, 201, 222
- Unno, W. 1955, *PASJ*, 7, 81
- Verner, D. A., Ferland, G. J., Korista, K. T., & Yakovlev, D. G. 1996, *ApJ*, 465, 487
- Weymann, R. J. & Williams, R. E. 1969, *ApJ*, 157, 1201

Table 1. Adopted Atomic Parameters<sup>a</sup>

transition	$\lambda$ (Å)	$f_{ul}$	$A_r$ (s <sup>-1</sup> )	$1 - \epsilon$
O VIII Ly $\alpha_1$	18.96711	$2.77 \times 10^{-1}$	$2.58 \times 10^{12}$	1.000
O VIII Ly $\alpha_2$	18.97251	$1.39 \times 10^{-1}$	$2.58 \times 10^{12}$	1.000
N VII Ly $\zeta$	18.97413	$4.81 \times 10^{-3}$	$2.97 \times 10^{10}$	0.797

<sup>a</sup>Wavelengths are adopted from Garcia & Mack (1965) and Johnson & Soff (1985). All other parameters are calculated with FAC (Gu 2003).

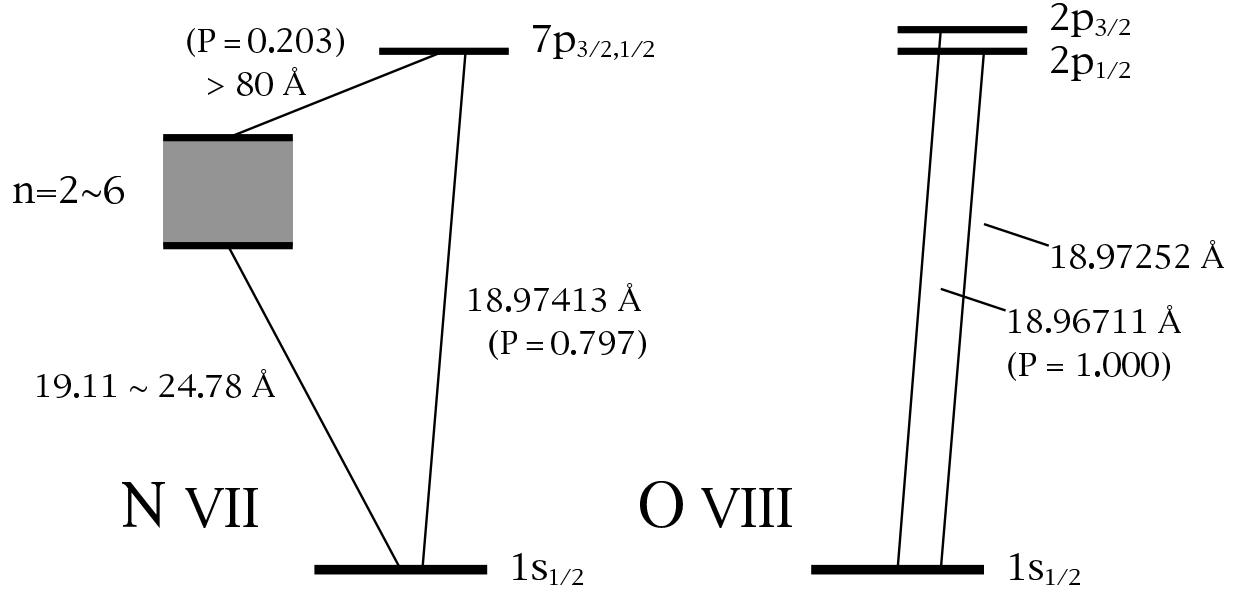


Fig. 1.— Partial Grotrian diagrams of the O VIII and N VII transitions relevant for the X-ray Bowen fluorescence mechanism. The probabilities for each channel  $P \equiv 1 - \epsilon$  are indicated.



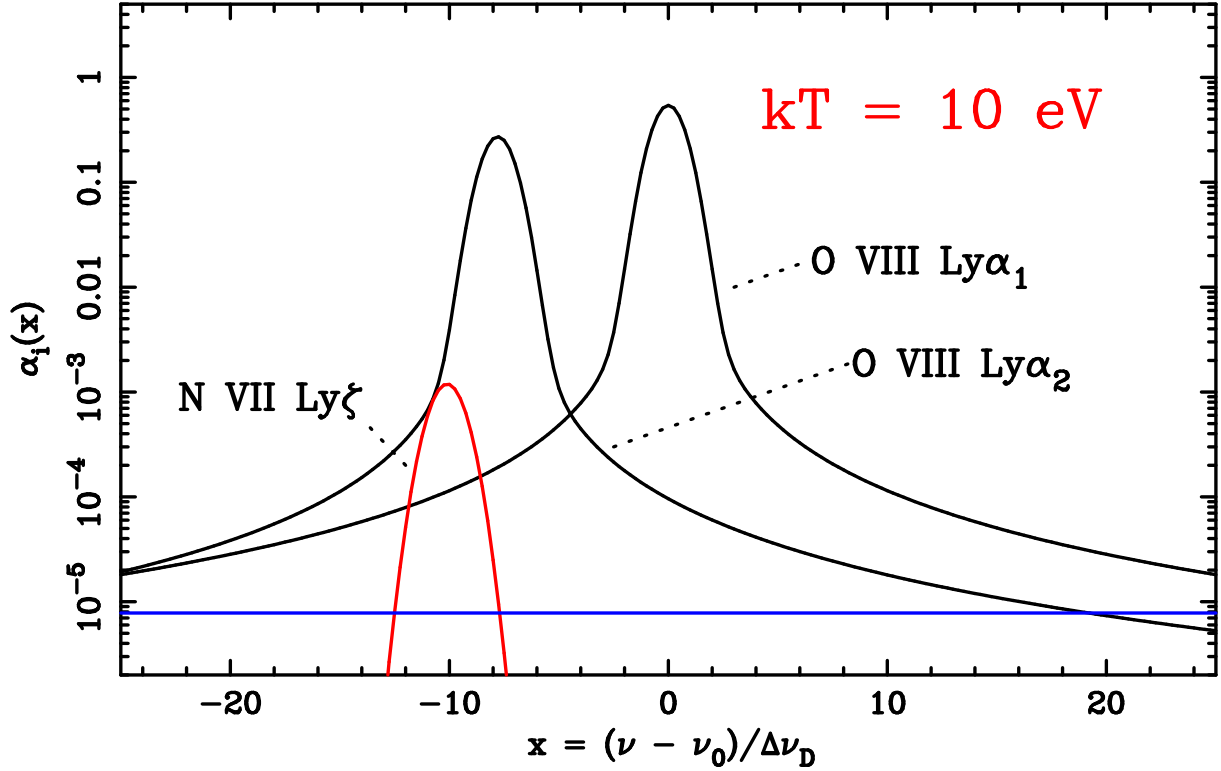


Fig. 2.— Normalized cross sections of as functions of the frequency for O VIII Ly $\alpha$  and N VII Ly $\zeta$  at a temperature of 10 eV. The frequency is expressed in multiples of the Doppler width of the O VIII Ly $\alpha_1$  line. The nitrogen to oxygen abundance ratio is assumed to be 0.13. The continuum absorption cross section is set to the value of  $\beta$  that corresponds to a column density of  $\tau_c = 0.1 \tau_{\text{O VIII}}$ .

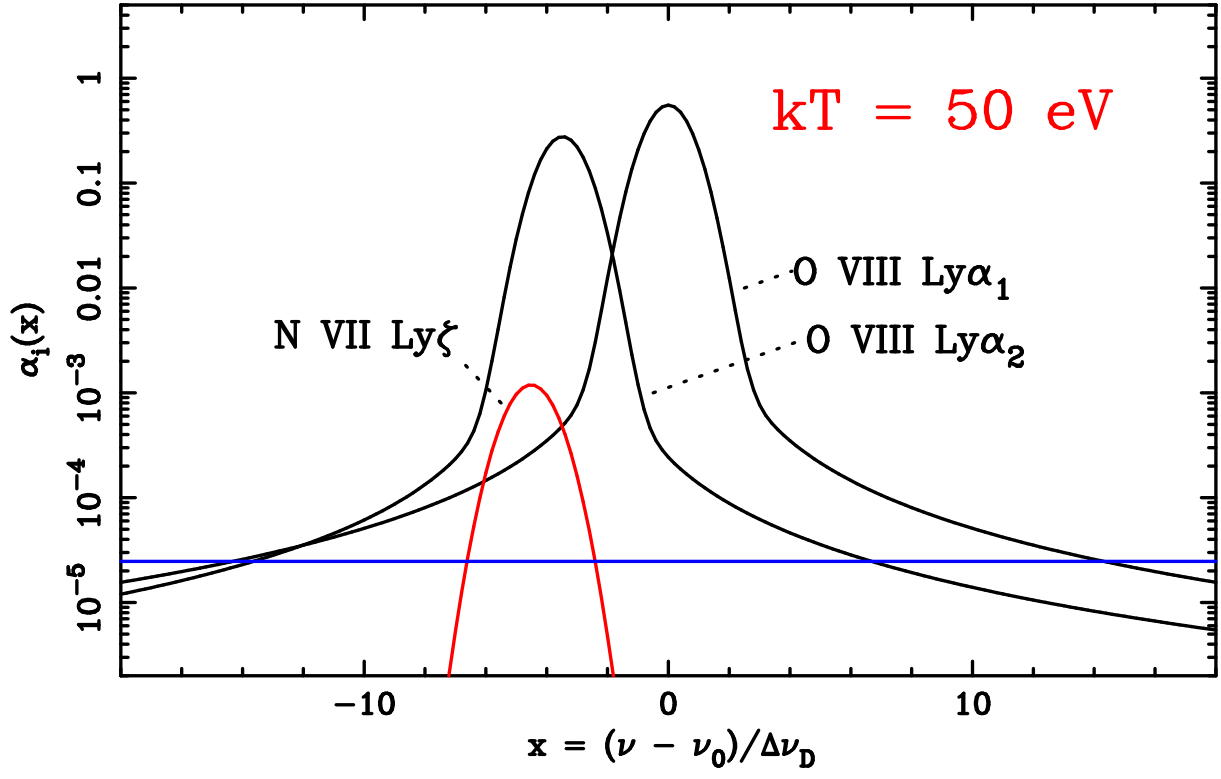


Fig. 3.— Same as in Figure 2 at a temperature of  $kT = 50$  eV.

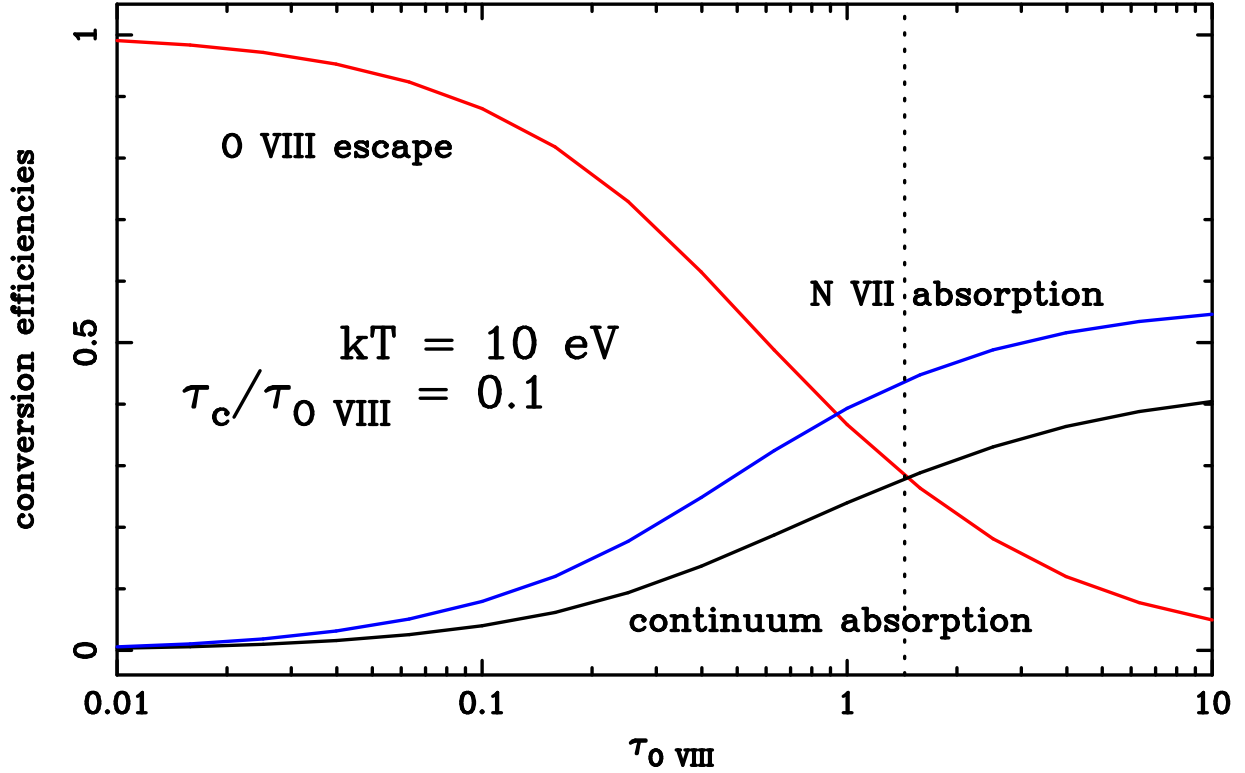


Fig. 4.— Fraction conversion efficiencies at  $kT = 10 \text{ eV}$  as a function of the total optical depth of the slab expressed in units of the threshold photoelectric opacity of O VIII. The underlying continuum opacity is fixed to be  $\tau_c = 0.1 \tau_{\text{O VIII}}$ . The frequency dependences of the line cross sections are shown in Figure 2. The vertical dotted line denotes where the O VIII Ly $\alpha_1$  line-center optical depth is  $10^4$ .

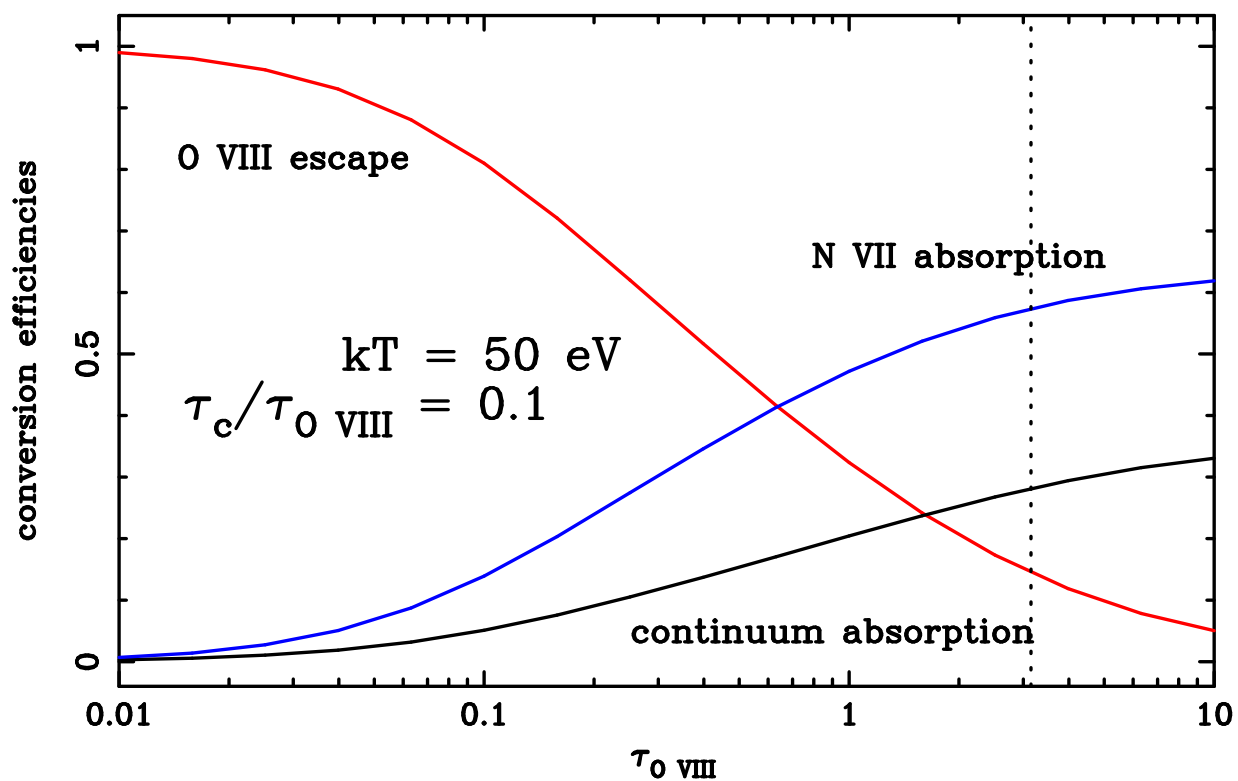


Fig. 5.— Same as in Figure 4 at  $kT = 50 \text{ eV}$ . The frequency dependences of the line cross sections are shown in Figure 3.

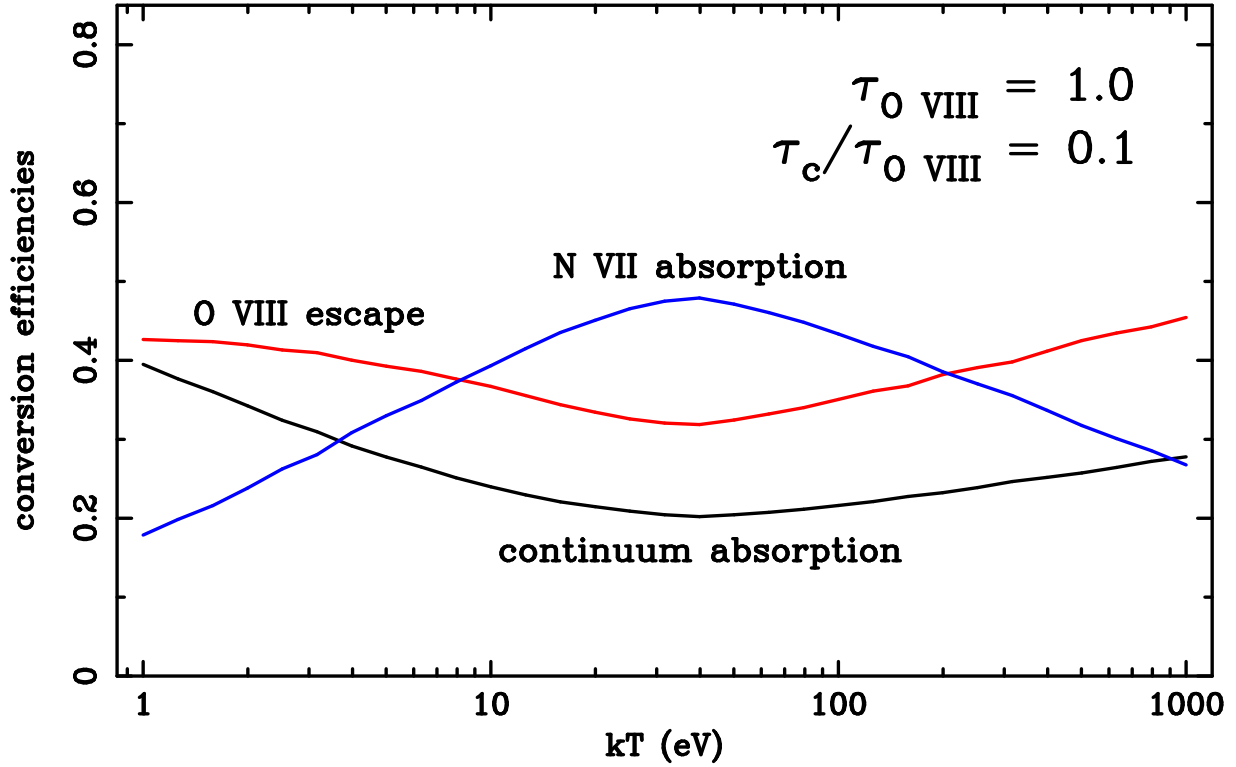


Fig. 6.— Temperature dependence of the fractional conversion efficiencies. The column density is fixed such that  $\tau_{\text{O VIII}} = 1.0$  and  $\tau_c = 0.1 \tau_{\text{O VIII}}$ . Conversion into N VII peaks at a temperature of  $kT \sim 40$  eV, which corresponds to the temperature where the separation between the O VIII  $\text{Ly}\alpha_2$  and N VII  $\text{Ly}\zeta$  lines is approximately one Doppler width (see text).

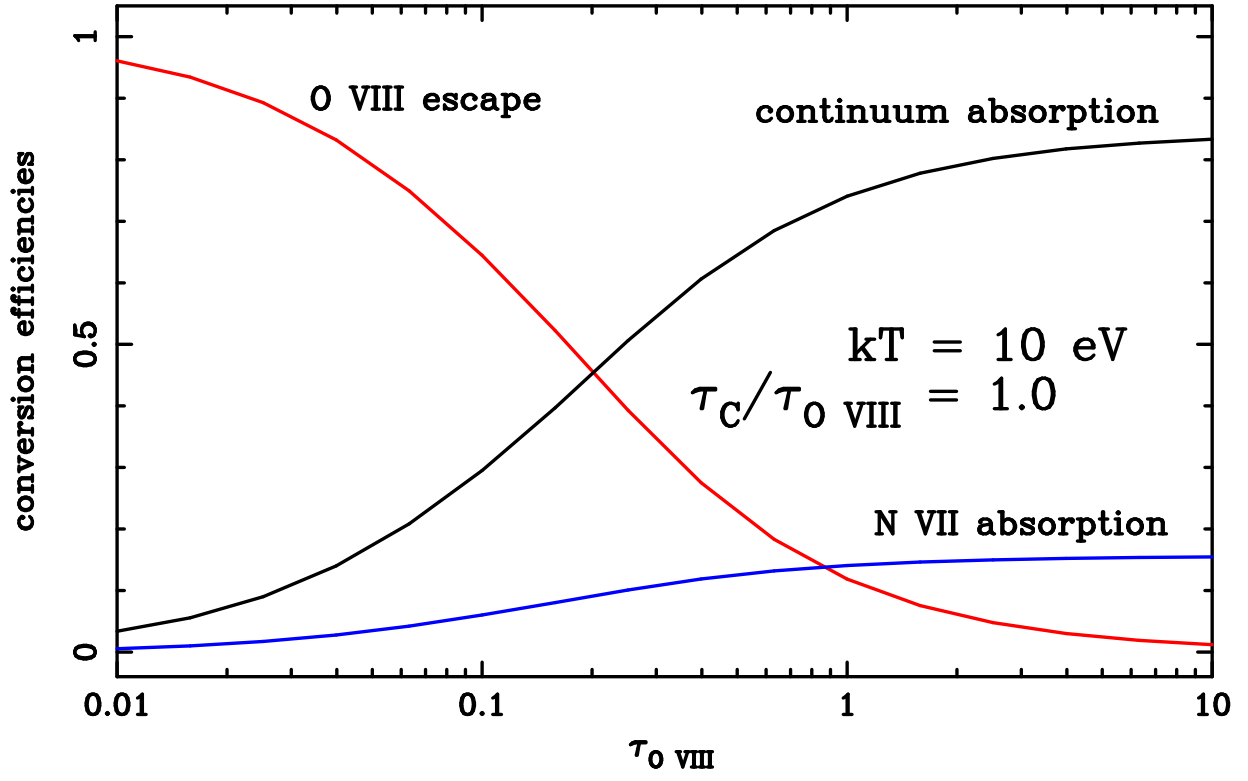


Fig. 7.— Same as in Figure 4 with the continuum opacity increased by a factor of 10 ( $\tau_c = \tau_{\text{O VIII}}$ ). In this case, continuum absorption dominates over line absorption by N VII.